ADVANCED FUNCTIONAL MATERIALS
www.afm-journal.de

Borax-Mediated Formation of Carbon Aerogels from Glucose

Tim-Patrick Fellinger, Robin J. White, Maria-Magdalena Titirici, and Markus Antonietti*

Hierarchically structured carbon aerogels are produced in a simple, rapid, efficient, and sustainable hydrothermal approach, using only glucose as the carbon precursor. Using sodium borate (borax) as a novel complex structure directing agent nanostructured, carbon monoliths, structurally similar to the well-known sol-gel monoliths made of silica are obtained. Experimental results indicate the acetalization reaction of monosaccharides with their dehydration product hydroxymethylfurfural to be very important and inhibiting in the process of hydrothermal carbonization. Addition of borax, leads to a competitive complexation of diols, resulting in promising secondary catalytic effect with regard to carbon yield. Accordingly, it is shown that the sugar:borax ratio directs the primary carbon nanoparticle size into the sub −50 nm range, while their spinodal destabilization ultimately results in the controlled aggregation of carbonaceous particles leading to the formation of monoliths in a simple one step hydrothermal process. Post-synthesis thermal carbonization is also used to increase surface area to the medium-high range, introducing electric conductivity into the carbon monoliths. The resulting materials are promising candidates for applications in flash chromatography, for fast adsorption/purifications, and as porous conductive electrodes.

1. Introduction

Aerogels are known in a great variety of compositions and are used in a manifold of high-end applications including chromatography, adsorption, separation, gas storage, detectors, heat insulation, as supports and ion exchange materials.[1–3] In this regard, silica aerogels are the most prominent and developed materials in this field, as they have revolutionized HPLC, allowing highest resolution and fast separation at the same time.[1] Silica however also has some chemical disadvantages, Pekala et al. in 1987, described the first organic aerogels as an interesting alternative.[2]

The formation of colloidal gels is a "bottom up" synthetic process following the well established sol-gel chemistry where colloidal particles form at first and then are aligned and condensed by thermodynamic forces.[3] Hierarchically structured, inexpensive porous organic aerogel examples are capable of competing with their inorganic (e.g. silica) counterparts in sorption and insulation applications.[4,5] The most common organic aerogels are based on resorcinol-formaldehyde mixtures (RF). Here the formation of the gel phase occurs through the catalyzed polycondensation of the reactive precursors in water.[2] While reactions free of catalyst lead to precipitation of micrometer sized particles,[6] a gel composed of small particles can be achieved either by acid or base catalysis. The particle size is decreasing with increasing relative amount of catalyst. The whole gel formation can take several days. The gel cross-links throughout the whole volume, whilst the amount of solvent directly controls the final density or overall porosity. A well-developed microstructure is also crucial for the following drying procedure to achieve the organic aerogels. The solvent has to be removed from the pores, while the structure has to withstand capillary forces induced by evaporation. Some investigations on this topic have been summarized by Job et al.[7] So far supercritical drying is still the most prominent procedure used to minimize the effects of capillary collapse.

Beside being highly porous and lightweight, another advantage of organic aerogels is the possibility to introduce electric conductivity by converting them into carbon aerogels, thus accessing electrical/electrochemical applications like batteries,[8] supercapacitors[9] and as conductive supports.[10] For those applications, it is important to have additional control of the well-developed micro- and mesoporosity. As it is possible to subtly influence and design material nanoscale structuring by chemical means, such carbon aerogels can also be classified as nanostructured carbon.[11] To convert polymer into carbon aerogels, usually pyrolysis above 600 °C is employed. The carbonization process leads to a loss of oxygen and hydrogen functionalities and therefore more condensed carbon structures.[11,12] Finally, depending on the pyrolysis temperature and the respective precursor chemistry ("graphitizability") of the former organic structure, an electrically conductive carbon network is achieved and can be used for a wide range of applications. A review article on RF-based organic and carbon aerogels was published by Al-Muhtaseb et al.[13]

Dr. T.-P. Fellinger, Dr. R. J. White,
Dr. M.-M. Titirici, Prof. M. Antonietti
Max-Planck-Institut für Kolloid-und Grenzflaechenforschung
MPI Campus Golm
Am Muehlenberg 1, 14476 Potsdam- Golm, Germany
E-mail: Fellinger@mpikg.mpg.de

DOI: 10.1002/adfm.201102920

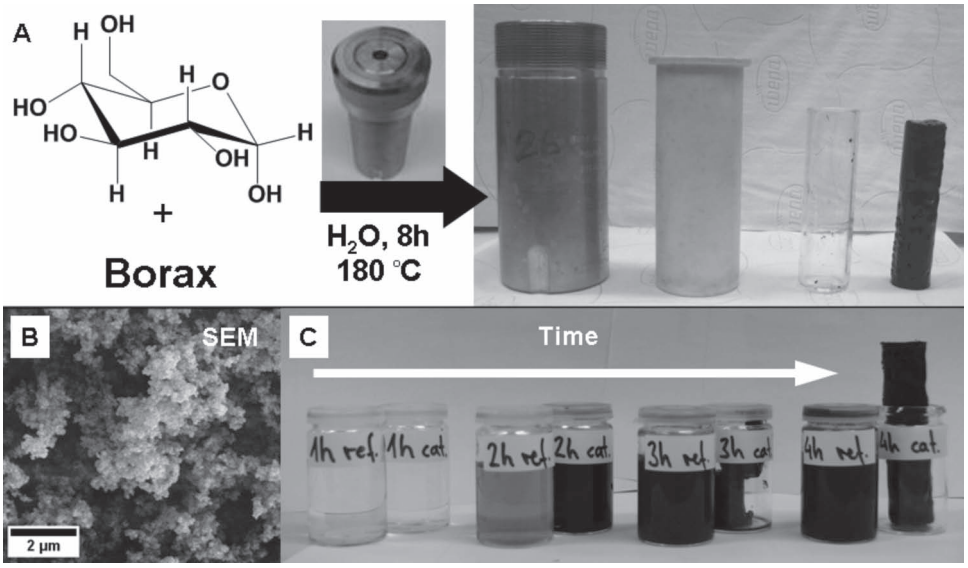

Figure 1. A) Schematic presentation of the hydrothermal carbonization (HTC) process to obtain gels. B) SEM image showing a composition of small aggregated particles. C) Illustration of radically reduced reaction times compared to classical HTC of glucose. Shown are results from 20 mL glucose solutions (30%) with (cat.) and without (ref.) the addition of 500 mg of borax for 1, 2, 3, and 4 h at 200 °C.

Regarding the synthesis and use of such carbon aerogels, there is however still unexploited potential. This is partly due to the restricted chemical variability of RF resins, but also due to the fact that resorcinol and formaldehyde are harmful chemicals. A more flexible, green and sustainable approach requires the use of renewable resources and a less harmful synthesis,[14] and carbon aerogels are to be generated from inexpensive biomass-derived precursors, serving both the economic and ecologic point of view.[15] Herein the production of monolithic functional carbonaceous gels possessing astonishing physicochemical similarity to the state-of-the-art RF gels, however prepared from inexpensive, harmless and naturally available compounds in one step using the process of hydrothermal carbonization (HTC) is presented. These carbon aerogels can then be simply treated thermally under an inert atmosphere to alter surface chemistry and structural properties.

Using this well-established method in sustainable chemistry (i.e. autoclave-based HTC) we have demonstrated previously the accessibility of rather hydrophilic carbonaceous material composed of micrometer-sized spherical particles from carbohydrate biomass under self-generated pressure by an exothermic reaction at temperatures of 180–200 °C.[16,17] Material formation involves dehydration of sugars (to form 5-hydroxylmethylfurfural (HMF) in the case of glucose/fructose), condensation and polymerization but also aromatization, leading to a coal-like product.[18] However for most technology important applications (e.g. heterogeneous catalysis, electrodes, sorption etc.) higher surface area and porosity of the carbonaceous product are essential. In this context bottom-up approaches using metal salts,[19] surfactants,[20–22] hard templates[23] and other additives[24] have successfully resulted in the formation of nanostructured carbon or carbon composite materials demonstrating their general feasibility. However all the attempts utilize chemicals making the process less green or facile and to the best of our knowledge there is still no simple route which allows subtle control over textural properties (e.g. surface area) and the ability to tailor pure hydrothermal carbon particle size to < 50 nm diameter.

Herein we observe that borax ($Na_2B_4O_7$) acts both as a catalyst and structure-directing agent. Concluding from the changed reactivity via the employment of borax we propose a mechanism, which also touches the production of HMF as sustainable platform chemical. However our focus is extending the HTC process to the nano-range and allowing sol-gel manufacture of sustainable carbon aerogels. By employing HTC in combination with borax, the formation of gels composed of aggregated spheres with a significantly decreased particle size (as compared to conventional hydrothermal carbon) in radically reduced reaction times is possible (**Figure 1**). Analogous to previous aerogel recipes, experimental parameters can be adjusted to control both material micro- and nanostructure, as particle size depends on the ratio of sugar/borax while porosity depends on overall concentration. Similarly to traditional RF-based systems, the presented HTC hydrogels can be dried via diverse routes (e.g. evaporative drying, supercritical CO_2 extraction or freeze drying) to achieve HTC aerogels, which can be post-carbonized to carbon aerogels, referred to here under the generic term "carbogels".

2. Results and Discussion

Representative of our reported system, four carbogels examples were synthesized at different sugar/borax ratios denoted as carbogels X, where X corresponds to the used amount of borax in milligrams while the amount of water and glucose was kept the same. The carbogels were produced by hydrothermal treatment of the solutions at 180 °C for 8 h (Figure 1). Shorter reaction

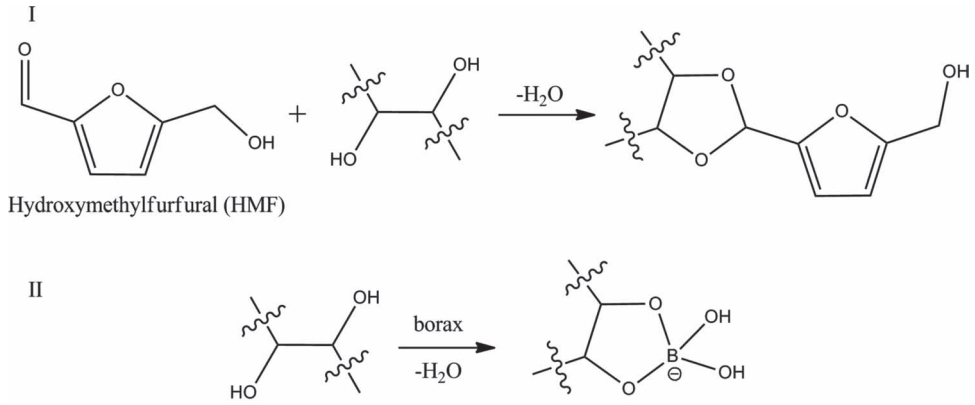

Figure 2. Side reactions (I acetalization; II borate-diol complexation) within the hydrothermal carbonization of sugar (herein simplified as dioles) in the presence of borax.

times resulted in the formation of unstable gels or sol-like suspensions (Figure 1). Both with increasing concentration of borax and longer reaction times, mechanically stable and brown to black-colored monoliths were received (Figure S1, Supporting Information). Non-incorporated soluble compounds including boronic compounds such as borax (confirmed by inductively coupled plasma optical emission spectrometry (ICP-OES) and wide angle X-ray diffraction (WAXS) were then removed by H_2O and ethanol washing, followed by further washing with excess H_2O prior to freeze drying. Under the reported reaction conditions, low density (e.g. $\rho \sim 0.12$ g cm^{-3}) light brown to black colored carbogels are produced of ca. 3.1 g mass with a carbon content of ~64% (thus resulting in 73% carbon yield with respect to glucose, the volume fraction of pores is $\Phi \approx 0.94$). Mechanistically, the role of borax in our system appears to be rather complex. The accelerated carbonization by borax, i.e. higher yields in shorter times with an onset at lower temperatures, cannot only be explained by catalysis of glucose dehydration via accelerated isomerization to fructose, reported by Riisager et al.[25,26] First, under hydrothermal conditions the Lobry de Bruyn-Berta van Ekstein isomerization already converts glucose into fructose.[27] Second, the dehydration is not a rate-limiting step in the reaction cascade of hydrothermal carbonization and third borax also shows a catalytic effect on the conversion of fructose (see Supporting Information). Therefore, a more detailed view into the formation mechanism is needed to understand the impact of borax. The fact that the particle size found is even smaller as compared to HTC of pure HMF corroborates this statement. Starting from high glucose concentrations the reaction of readily formed HMF with sugars instead of condensation/polymersization is the most probable. In the industrial synthesis of furfural, a famous derivative of HMF, from pentoses, not the whole sugar is converted to furfural. An important yield lowering reaction is known to be the acetalization of pentoses with furfural.[28] Acetal formation from HMF with glucose and/or fructose, as well as intermediate diols can be expected. Indeed, hydrothermal carbonization of equimolar amounts of HMF and a HMF/glucose mixture at 180 °C for 11 h lead to different solid yields (yield (HMF) > yield (mixture)), although the time scale of dehydration are minutes.[29] The acetalization leads to a protection and therefore reduced reactivity of the HMF formyl group (**Figure 2**/I). In agreement with the interpretation of Riisager et al. we propose that the interaction of borax with sugar diols forms negatively charged complexes, catalyzing the isomerization to fructose, which can be dehydrated more easily as compared to glucose (Figure 2/II). Extending the previously reported work of Riisager et al., we propose the complex formation to compete with the acetalization, leading to an increased formation of the free HMF and overall reactivity.

The formation of gels from pure HMF in the presence of borax is indicative of borax additionally promoting interpolyfurane chain cross-linking, potentially *via* boron didiol complex initiated "template effect", which is essential for the gelation process. It is to be mentioned that the borax salts are not permanently bound to the surface in the final product and can be easily washed out at the end of the process, essentially to be recycled for the next carbogel reaction. Scanning and transmission electron microscopy (SEM/TEM) image analysis of the resulting aerogels revealed the presence of very small, spherical HTC nanoparticles, aggregating to create a gel structure with hierarchical porosity, with the particle size distribution being much smaller, narrower and well defined as compared to previously reported, standard HTC products (**Figure 3**). With increasing system borax concentration, the microstructure becomes increasingly finer due to a decrease in primary particle size (Figure 3). Here the borax-mediated enhanced reactivity essentially originates an increased number of nucleation seeds by burst nucleation. The particle diameter of Carbogel-100 was calculated as ~41 nm, decreasing to less than ~7 nm with increasing borax concentration (e.g. carbogel-750; **Table 1**). Both SEM and TEM images reveal the carbogel network to be composed of monodisperse, aggregated, spherical nanoparticles generating the desired hierarchical porous network, well suited for use in catalysis, electrochemical applications (e.g. electrocatalysis, batteries and supercapacitors) or chromatography, where fast mass transport through the pore system plays a crucial role. It has to be mentioned that the gel structure shrinks at lower sugar/borax ratios throughout freeze-drying, indicating that the more fragile, 7 nm thick carbon walls cannot withstand the higher capillary pressures. Note that with an overall downscaling of the structure the wall stability is less, while the capillary pressures increase.

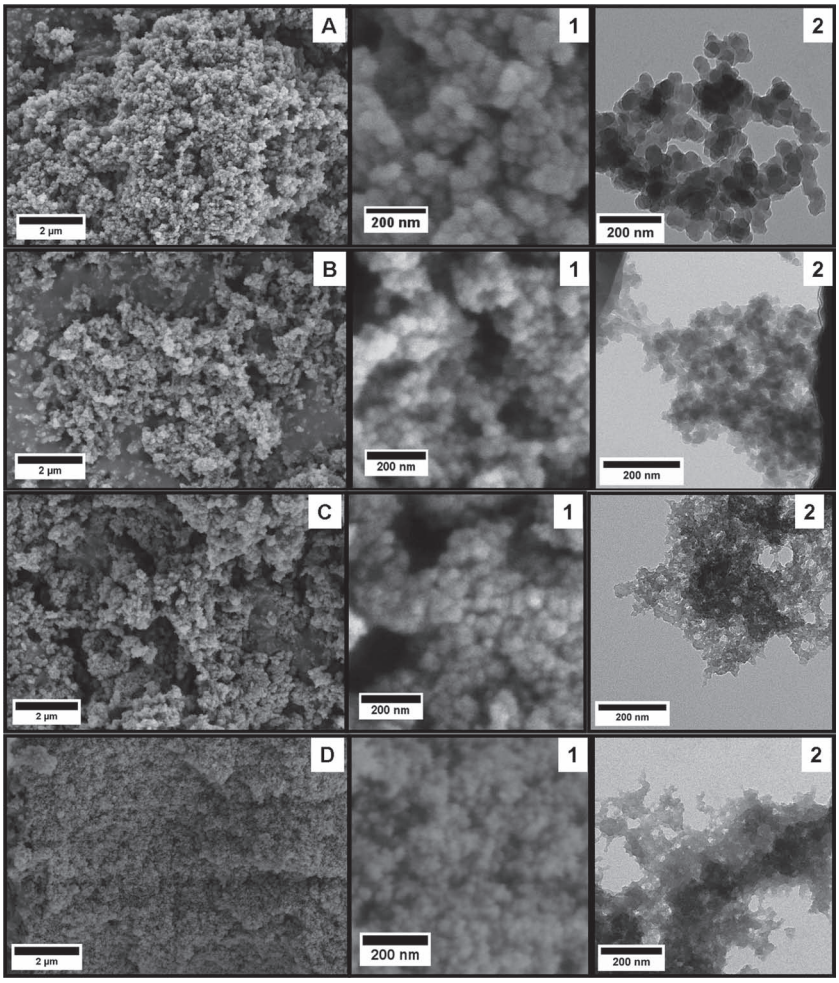

Figure 3. SEM and TEM images of Carbogels-*X* prepared from different amounts *X* of borax (in mg), with the same amount of water and glucose. SEM overview images are presented on the left side, while the respective higher resolution SEM and TEM images are indicated as 1 and 2.

Thermal treatment of the dried hydrophilic aerogels under a non-oxidative atmosphere (i.e. N_2) at 550 °C and 1000 °C (heating rate = 10 K min^{-1} followed by an isothermal period of 5 h) leads to uniform dimensional shrinkage of the monolith macrostructure with preservation of the overall cylindrical shape. At higher sugar/borax ratios the local nano- and microstructure in terms of particle shape and connectivity are also retained upon heating to these carbonization temperatures (**Figure 4**). However, aerogels composed of very fine, sub-10 nm particles do not completely withstand the carbonization process and shrink to more condensed systems. Determination of the particle size via TEM (Figure 4/carbogel 750 at 1000 °C) indicates that also the primary particle size decreases upon carbonization, in accordance with the mass loss throughout carbonization. Elemental analysis indicates the loss of oxygen and hydrogen from the carbonaceous material structure, with carbon content increasing from ~64 wt% (as-prepared) to ~94 wt% (at 550 °C) and ~97 wt% (at 1000 °C).

In addition, nitrogen sorption measurements were carried out to investigate the porosity of the as formed hierarchical carbon structures (Table 1). With increasing sugar/borax ratio, the aerogels show an increasing gas uptake and a higher specific surface area due to the presence of smaller primary nanoparticles. Carbogel-750 breaks this trend, as the BET value of 209 $m^2 g^{-1}$ is decreased compared to 233 $m^2 g^{-1}$ for carbogel-500. In accordance with the TEM images (Figure 3D), this reflects the collapse of the very fine structure within the freeze drying process, i.e. 7 nm disordered carbon cannot withstand the capillary forces of a pore of similar size. This is well known from corresponding, even rigid polymer structures.[30]

Regarding gas sorption behavior for the post-carbonized systems, a strong increase of the specific surface area especially after thermal treatment at 550 °C/N_2 is observed. High surface area materials with ~600 $m^2 g^{-1}$ (carbogel-250 at 550 °C) are accessible even without chemical activation using the relatively simple synthetic route

Table 1. Specific surface area and particle size (TEM) for representative carbogels prepared at 180 °C and material post-carbonized at 550 °C and 1000 °C.

Sample Name	180 °C		550 °C		1000 °C	
	S_{BET}[a] [$m^2 g^{-1}$]	Particle diameter[b] [nm]	S_{BET}[a] [$m^2 g^{-1}$]	Particle diameter[b] [nm]	S_{BET}[a] [$m^2 g^{-1}$]	Particle diameter[b] [nm]
Carbogel-100	84	41	491	33	275	28
Carbogel-250	208	22	614	18	360	13
Carbogel-500	233	12	458	14	206	13
Carbogel-750	209	8	403	12	205	–

[a]Specific surface area from BET method; [b]Diameters calculated in Image J software from TEM images.

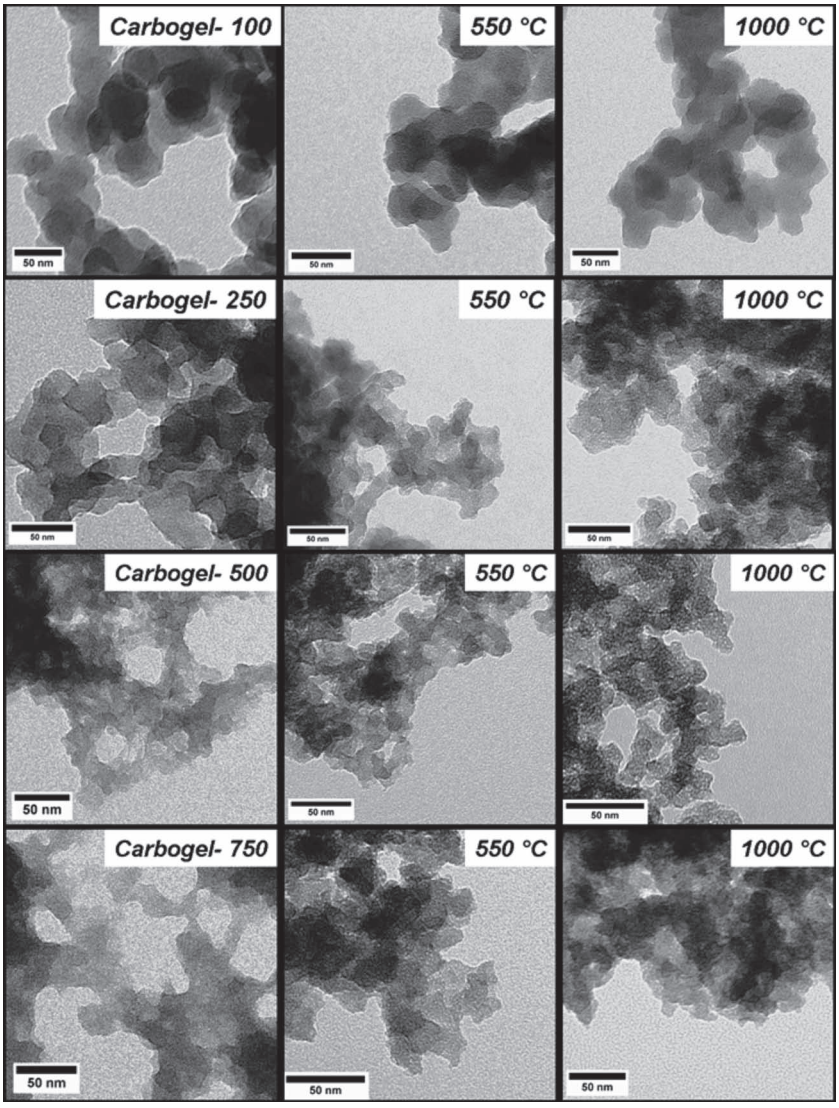

Figure 4. Comparison of TEM images of as-prepared carbogels-*X* (left) and the respective post-carbonized samples at 550 °C (middle) and 1000 °C (right), where *X* stands for the used amount of borax within the synthesis protocol.

and conditions. The carbonized carbogel-100 and carbogel-250 samples again show a trend of increasing surface area with increasing sugar/borax ratio, the result of a reduction in the primary particle size. The high borax structures are again already too fine to withstand carbonization completely, resulting in partial structure collapse and a marked reduction of the accessible surface and overall porosity. The interplay of enhancement of surface area and fragility of the architecture is also nicely reflected in the high temperature data: carbonization at higher temperatures (i.e. 1000 °C) produces lower surface area materials, although the primary particle size has been dramatically decreased.

A more quantitative porosimetry analysis of the optimal products, carbogel-250 and the corresponding post-carbonized carbogels, was performed (**Table 2**; **Figure 5**). Only marginal hysteresis and lack of defined plateau region as relative pressure reaches unity (i.e. $p/p_0 \sim 1$) of the sorption profile, reflects the combination of a slit-type micropore structure combined with a high external surface area due to small, interconnected primary carbon nanoparticles (Figure 5).

The exploding sorption capacity at relative pressures near unity reflects the presence of excessive large diameter mesoporosity and macroporosity, which can be expected from a material with 94 vol% overall porosity.

As-prepared carbogels show in general limited microporosity ($V_{micro} \leq 0.10$ cm^3 g^{-1}; Table 2), which is very typical for ductile, polymer-like behavior of the walls.[30] Heat treatment at 550 °C significantly increases this micropore content to about 0.25 cm^3 g^{-1}, which means that the material now behaves as a rigid carbon scaffold post-carbonized carbon aerogels showing isotherms (left) and pore size distributions (right).

Also the mesopore volume is observed to increase nicely upon carbonization at 550 °C ($V_{meso} > 0.5$ cm^{3}g^{-1} @ 550 °C; Table 2), most likely as the result of material contraction/condensation processes which open up interstitial porosity between the primary particles, which was closed ahead by ductile deformation. Interestingly, N_2 sorption at carbogel-250 at 1000 °C shows a loss both of micro- and mesoporosity. This means that the structure rearrangements

Table 2. Nitrogen sorption data and electrical conductivity for carbogel-250 prepared at 180 °C and post-carbonized at 550 °C and 1000 °C.

Sample Name	S_{BET}[a)] [m^2 g^{-1}]	Pore Volume[b)] [cc g^{-1}]	Micropore volume[b)] [cc g^{-1}]	Mesopore volume[b)] [cc g^{-1}]	APD[b)] [nm]	Specific conductivity[c)] [S m^{-1}]
Carbogel-250 @ 180 °C	208	0.43	0.10	0.34	1.56	0.7 10^{-3}
Carbogel-250 @ 550 °C	614	0.81	0.24	0.57	0.82	60
Carbogel-250 @ 1000 °C	360	0.54	0.18	0.36	2.18	290

[a)]Specific surface area from BET method; [b)]Pore size characteristics obtained via the QSDFT model; [c)]Potentiostatic electrochemical impedance spectroscopy (1–1000Hz; R-Model).

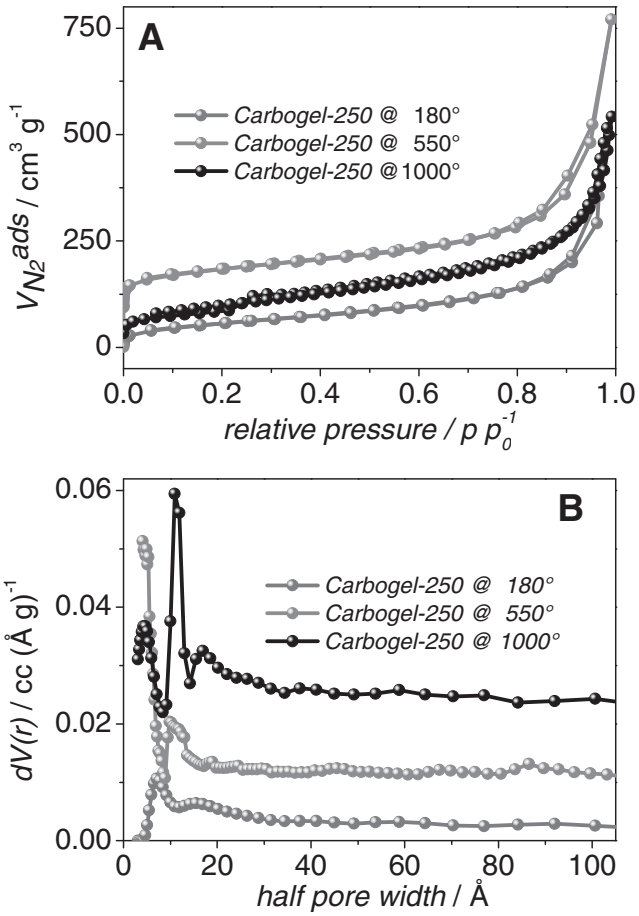

Figure 5. Comparison of nitrogen sorption isotherms (A) and pore size distributions (B) of as-prepared carbogel-250 and the respective post-carbonized samples at 550 °C and 1000 °C, where X stands for the used amount of borax within the synthesis protocol.

observed by TEM on a larger scale are also found on the molecular and few nanometer scale: the whole structure simply sinters due to temperature induced carbon-carbon rearrangements.

To investigate the applicability in electrochemical applications i.e. as electrode materials in various systems, we also measured electrical conductivities of pulverized and pressed carbogel-250 before and after thermal treatment under inert atmosphere. As seen in Table 2, the specific conductivities increase with increasing carbonization temperature reaching 290 S m^{-1} at 1000 °C. These values are, considering the extremely high porosity of the materials, comparably high and absolutely sufficient to support an electrode application.

The hierarchical porosity of the monolithic carbogels suggest the use of the material as electrodes for fast processes, were mass transport takes a crucial role. The presented synthesis lays the basis for the development of a wide range of useful sustainable carbon-based nanotechnology. Future research will deal with further manipulation of porosity/surface area properties and the further improvement of stability in the low nanometer-range against drying/carbonizations steps as this will further improve the materials applicability.

3. Conclusions

In summary our synthesis is a simple, sustainable and scalable route to the preparation of carbogel materials with similarities to more traditional resorcinol-formaldehyde (RF) based organic aerogels, in terms of parameters for controlling the nanostructure and porosity. Borax has the equivalent catalyzing impact on hydrothermal carbonization of glucose as traditional acid/base catalysts employed in the RF system. Experimental results suggest the important role of acetal formation from the reaction of the formyl group of HMF with the diol subunit of sugars in hydrothermal treatment of carbohydrates e.g. glucose. Addition of borax leads a competitive reaction to the HMF-deactivating acetalization and therefore results in a catalytic effect, which can be used for the variation of particle size just as in the RF system. Complete recovery of borax and further carbonization of the freeze dried gels allows morphological control and the facile generation of conductive, pure carbon aerogels with high specific surface areas/volumes; features which have thus far been missing from previously reported template-free HTC routes. We regard this as a competitive, green and economical way to promising, functional, utile, porous carbon materials. Regarding the strong micropore evolution at moderate carbonization temperatures (e.g. 550 °C) we want to emphasize the easy and fast bottom-up generation of high surface area material without additional (chemical) activation using the HTC additive mineral borax.

4. Experimental Section

All used chemicals were purchased at Sigma-Aldrich Co. and used as received. Representing our system, five exemplary carbogels were synthesized at different sugar/borax ratios denoted as carbogels *X*, where *X* corresponds to the amount of borax in milligrams, respectively dissolved in 15 mL distilled water with 6.5 g of D-glucose. These solutions were prepared in a quartz tube, then placed in a Teflon-lined autoclave and sealed. The mixtures were then heated to 180 °C for 8 h under self-generated pressure in this closed system. Black-colored and mechanically stable monoliths are then recovered (Figure S1, Supporting Information). Non-incorporated soluble compounds, including boronic compounds such as borax, were extracted first with H_2O and then with ethanol (3 × 50 ml for one day). After purification and changing the solvent back to water the samples were freeze dried resulting in 3.1 g (80% carbon yield) low density ($\rho \sim 0.12$ g cm^{-3}) carbogels of a light brown to black color. Particle morphology/size was visualized using a Gemini scanning electron microscope (SEM). Transmission electron microscopy (TEM) was carried out with Carl Zeiss Omega 912X at an acceleration voltage of 120 V. Particle size was measured applying Image J software on optimally resolved images. N_2 sorption analysis was performed at 77 K using a QUADROSORB SI, equipped with automated surface area and pore size analyzer. Before analysis, samples were degassed at 150 °C for 20 h using a masterprep degassing system. Specific surface areas were determined BET method. Pore size distributions were determined by the QSDFT model and the N_2 adsorption isotherm. Electrochemical measurements were carried out with Gamry Reference 600 potentiostate (Gamry Instruments) and Gamry EIS 300/Physical Electrochemistry software. Electrical conductivity was achieved applying R-model on

potentiostatic impedance spectroscopy at 1-1000 Hz using a two electrode setup. FT-IR spectra were recorded with ATR method using a Varian 600 FT-IR Spectometer. Elemental composition was measured with a Vario El elemental analyser.

Supporting Information

Supporting Information is available from the Wiley Online Library or from the author.

Acknowledgements

The authors are grateful to the ERC Senior Excellence Program, the EU project Hydrachem and the Max Planck Society for financial support. Special thanks go to M. Alnaief, Prof. I. Smirnova (Technische Universität Hamburg-Harburg) and C. Falco for performing $ScCO_2$ drying and SEM measurements.

Received: December 2, 2011
Revised: February 3, 2012
Published online: April 23, 2012

[1] K. Nakanishi, H. Minakuchi, N. Soga, N. Tanaka, *J. Sol-Gel Sci. Technol.* **1998**, *13*, 163.
[2] R. W. Pekala, *J. Mater. Sci.* **1989**, *24*, 3221.
[3] K. J. Klabunde, R. M. Richards, *Nanoscale Materials in Chemistry*, Wiley-VCH, Weinheim **2009**.
[4] H. Kabbour, T. F. Baumann, J. H. Satcher, A. Saulnier, C. C. Ahn, *Chem. Mater.* **2006**, *18*, 6085.
[5] X. Lu, M. C. Arduinischuster, J. Kuhn, O. Nilsson, J. Fricke, R. W. Pekala, *Science* **1992**, *255*, 971.
[6] R. Petricevic, G. Reichenauer, V. Bock, A. Emmerling, J. Fricke, *J. Non-Cryst. Solids* **1998**, *225*, 41.
[7] N. Job, A. Thery, R. Pirard, J. Marien, L. Kocon, J. N. Rouzaud, F. Beguin, J. P. Pirard, *Carbon* **2005**, *43*, 2481.
[8] M. Mirzaeian, P. J. Hall, *Electrochim. Acta* **2009**, *54*, 7444.
[9] M. C. Gutierrez, F. Pico, F. Rubio, J. M. Amarilla, F. J. Palomares, M. L. Ferrer, F. del Monte, J. M. Rojo, *J. Mater. Chem.* **2009**, *19*, 1236.
[10] J. Marie, R. Chenitz, M. Chatenet, S. Berthon-Fabry, N. Cornet, P. Achard, *J. Power Sources* **2009**, *190*, 423.
[11] P. F. Serp, J. L. Figueiredo, *Carbon Materials for Catalysis*, John Wiley & Sons, Inc., New York **2009**.
[12] H. Tamon, H. Ishizaka, *J. Colloid Interface Sci.* **2000**, *223*, 305.
[13] S. A. Al-Muhtaseb, J. A. Ritter, *Adv. Mater.* **2003**, *15*, 101.
[14] J. A. Dahl, B. L. S. Maddux, J. E. Hutchison, *Chem. Rev.* **2007**, *107*, 2228.
[15] D. C. Wu, R. M. Fu, *Microporous Mesoporous Mater.* **2006**, *96*, 115.
[16] M. M. Titirici, M. Antonietti, *Chem. Soc. Rev.* **2010**, *39*, 103.
[17] B. Hu, K. Wang, L. H. Wu, S. H. Yu, M. Antonietti, M. M. Titirici, *Adv. Mater.* **2010**, *22*, 813.
[18] M. Sevilla, A. B. Fuertes, *Chem.–Eur. J.* **2009**, *15*, 4195.
[19] X. J. Cui, M. Antonietti, S. H. Yu, *Small* **2006**, *2*, 756.
[20] Y. Yan, H. F. Yang, F. Q. Zhang, B. Tu, D. Y. Zhao, *Small* **2006**, *2*, 517.
[21] X. M. Sun, Y. D. Li, *J. Colloid Interface Sci.* **2005**, *291*, 7.
[22] Z. H. Wen, Q. Wang, Q. Zhang, J. H. Li, *Electrochem. Commun.* **2007**, *9*, 1867.
[23] S. Ikeda, K. Tachi, Y. H. Ng, Y. Ikoma, T. Sakata, H. Mori, T. Harada, M. Matsumura, *Chem. Mater.* **2007**, *19*, 4335.
[24] R. D. Cakan, M. M. Titirici, M. Antonietti, G. L. Cui, J. Maier, Y. S. Hu, *Chem. Commun.* **2008**, 3759.
[25] T. S. Hansen, J. Mielby, A. Riisager, *Green Chem.* **2010**, *13*, 109.
[26] T. Ståhlberg, S. Rodriguez-Rodriguez, P. Fristrup, A. Riisager, *Chem.–Eur. J.* **2011**, *17*, 1456.
[27] O. Bobleter, *Prog. Polym. Sci.* **1994**, *19*, 797.
[28] H. E. Hoydonckx, W. M. Van Rhijn, W. Van Rhijn, D. E. De Vos, P. A. Jacobs, in *Ullmann's Encyclopedia of Industrial Chemistry*, (Ed: B. Elvers), Wiley-VCH Verlag GmbH & Co. KGaA, Weinheim **2000**.
[29] F. Salak Asghari, H. Yoshida, *Ind. Eng. Chem. Res.* **2006**, *45*, 2163.
[30] A. Thomas, F. Goettmann, M. Antonietti, *Chem. Mater.* **2008**, *20*, 738.